Soft Matter

PAPER

View Article Online
View Journal | View Issue

Cite this: *Soft Matter*, 2024, **20**, 9614

Composite of knitted fabric and soft matrix. I. Crack growth in the course direction†

Fengkai Liu,[a] Xi Chen,[a] Zhigang Suo *[b] and Jingda Tang *[a]

A composite of a knitted fabric and a soft matrix enables applications that require low stiffness and high crack resistance. Examples include heart valves and stretchable strain sensors. Here we study processes of crack growth in such a composite under monotonic and cyclic stretch. We fabricate a composite using a knitted fabric of nylon yarn and an elastomer matrix of polycarbonate urethane. We precut a sample with a crack, monotonically stretch the sample, and observe the growth of the crack. The crack grows in the matrix as the yarn slips and breaks. The stretch is converted to energy release rate G. We identify two critical energy release rates, G_A and G_B. When $G < G_A$, the yarn does not slip, and the crack does not grow in the matrix. When $G_A < G < G_B$, the yarn slips but does not break, and the crack grows in the matrix stably and arrests when the stretch stops increasing. When $G = G_B$, the yarn slips and breaks, while the crack grows unstably. When the sample is subject to cyclic stretch, we observe analogous behavior of crack growth and arrest, as well as yarn slip and yarn break. However, the two critical values, G_a and G_b, are much smaller than the corresponding values under monotonic stretch.

Received 20th September 2024,
Accepted 20th November 2024

DOI: 10.1039/d4sm01114g

rsc.li/soft-matter-journal

1. Introduction

Biological tissues, such as skins and heart valves, consist of collagen fibers embedded in a matrix of proteoglycan and glycosaminoglycans.[1–3] The collagen fibers are crimped and form a network, while the matrix is soft. Such a tissue has a J-shaped stress–stretch curve.[4] When the stretch is small, the collagen fibers are crimped, and the modulus of the composite is small. When the stretch is large, the collagen fibers become de-crimped, and the stress–stretch stiffens steeply. The tissue also exhibits extraordinary fatigue resistance.[5]

These biological tissues have inspired the development of synthetic composites of fabrics and soft matrices.[6–10] Attention here is focused on fabrics in which yarns are made of a much stiffer material than the matrix, such that the yarns are regarded as being inextensible. Consider fabrics of two types: woven and knitted. Yarns in a woven fabric bend negligibly, so that the woven fabric is nearly inextensible in the directions of the yarns (Fig. 1a). The yarn in a knitted fabric bends substantially, so that the knitted fabric is stretchable[11,12] (Fig. 1b). This paper studies the composite of knitted fabric and soft matrix.

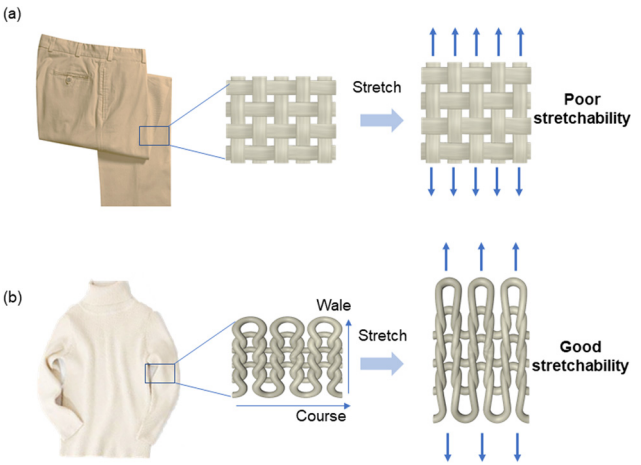

Fig. 1 (a) A woven fabric is nearly incompressible. (b) A knitted fabric is highly stretchable.

Such a composite has been developed as artificial muscles and strain sensors.[13] High tear resistance has been reported for knitted fabrics[14] and composites.[13]

Here we focus on the microscopic processes of crack growth in knitted fabrics and composites. Consider a knitted fabric consisting of a single yarn. A row of loops along the yarn is called a course, and a crack grows in the course direction by yarn slip and yarn break (Fig. 2a). A column of intermeshed loops is called a wale, and a crack grows in the wale direction by yarn ladder and yarn break (Fig. 2b). The crack growth in the

[a] State Key Lab for Strength and Vibration of Mechanical Structures, International Center for Applied Mechanics, Department of Engineering Mechanics, Xi'an Jiaotong University, Xi'an, China. E-mail: tangjd@mail.xjtu.edu.cn
[b] John A. Paulson School of Engineering and Applied Sciences, Kavli Institute for Bionano Science and Technology, Harvard University, Cambridge, MA, USA. E-mail: suo@seas.harvard.edu

† Electronic supplementary information (ESI) available. See DOI: https://doi.org/10.1039/d4sm01114g

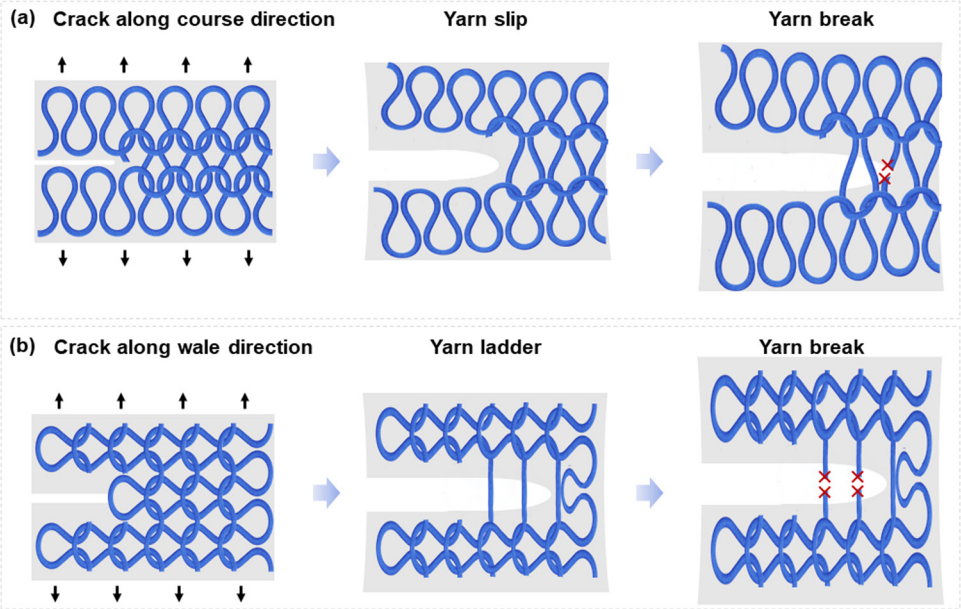

Fig. 2 (a) Crack in the course direction results in yarn slip and yarn break. (b) Crack in the wale direction results in yarn ladder and yarn break.

course direction is studied in this paper, and the crack growth in the wale direction will be reported in a subsequent paper.

The composite is prepared by embedding a nylon knitted fabric in a matrix of polycarbonate urethane (PCU). We precut a crack in a sample, in the course direction, and stretch the sample monotonically. The stretch is converted to the energy release rate, G. Two critical energy release rates are identified, G_A and G_B. When $G < G_A$, the yarn does not slip, and the crack in the matrix does not grow. When $G_A < G < G_B$, the yarn slips but does not break, while the crack grows and arrests. When $G = G_B$, the yarn slips and breaks, while the crack in the matrix grows unstably. Under cyclic stretch, the crack growth shows similar behaviors to monotonic stretching. However, the two critical energy release rates, G_a and G_b, are much reduced. It is hoped that this study will provide insight for designing novel woven structures[15] and fatigue-resistant soft composites for applications including artificial tissues, stretchable sensors.

2. Methods

2.1. Materials

Polycarbonate urethane (PCU) (Carbothane™ AC-4075A, Lubrizol, Wilmington, Massachusetts, M_w = 480 kDa). Tetrahydrofuran (THF) (Aladdin AR, 99.0%). Nylon knitted fabric was purchased from Fanjiati silk stocking company. The course direction has 26.3 unit cells per 1 cm, and the wale direction has 7.5 unit cells per 1 cm. Nylon woven fabric was purchased from Cloth Plus Fabric company. The warp direction has 9 unit cells per 1 cm, and the weft direction has 8.2 unit cells per 1 cm.

2.2. Preparation of knit-PCU composite and weave-PCU composite

We mixed 20 g of polycarbonate urethane (PCU) particles and 180 g of THF in a bottle, and stirred the mixture in a water bath at 60 °C for 2 hours. Then we cut a nylon knitted fabric or woven fabric into pieces of 90 mm × 140 mm × 80 μm. These pieces were immersed in a glass container with 20 g of PCU-THF solution. The glass container was subsequently placed in a fume cupboard overnight to let THF evaporate and PCU coat the fabric. The resulting sheet of composite had a thickness of 175.5 ± 10.4 μm. The weight ratio between the yarn and the PCU matrix is 44 wt%.

2.3. Optical microscopy observation

In this study, optical microscopy (RENYUE-4K) was used to observe crack propagation within the composite. This technique offers real-time visualization of micro-scale phenomena, allowing for detailed tracking of yarn slip and crack growth in the matrix.

2.4. Monotonic test

The toughness of the composite was measured using the pure shear test. Both intact and precut samples were cut into a rectangular shape with a width of 50 mm and height of 30 mm. The edges of the specimens were fixed to the acrylic sheet to ensure that the gauge height H was 10 mm. To prepare a precut sample, a sharp blade was used to create a 20 mm long cut at one side of the sample (Fig. S1, ESI†). All mechanical tests were performed using a tensile tester (SHIMADZU AGS-X) with a load cell of 1000 N and a stretching speed of 50 mm min^{-1}. All mechanical tests are conducted at about 25 °C. Every test was repeated for three times for assess repeatability and variations. Photos and videos during the test were captured using a microscope (RENYUE-4K). The modulus was calculated by the initial slope of the stress–stretch curve between the stretch of $\lambda = 1$ and $\lambda = 1.2$.

2.5. Cyclic test

The sample in the cyclic test had the same geometry as that used in the monotonic test. In one cycle, the sample was

stretched to a prescribed displacement and then unloaded. For samples without precut cracks, cyclic loads were applied to observe the change of stress–stretch curves. For precut samples, a camera was used to observe the propagation of the cracks. Both stretching and unloading were under a constant speed of 1 mm s^{-1}. A digital camera was used to take a sequence of photos every 15 minutes. For every sequence of photos, we selected the one near to the zero stretch and measured the crack length.

3. Sample preparation and stress–stretch curves

We dissolve polycarbonate urethane (PCU) particles in tetrahydrofuran (THF) solvent and submerge in the solution a knitted nylon fabric (Fig. 3a). After the solvent evaporates, the PCU coats the nylon fabric, forming a knit-PCU composite. The PCU matrix is transparent, and the nylon fabric is clearly visible under an optical microscope (Fig. 3b). The structure of the fabric does not change during the fabrication of the composite. We cut the composite and observe the cross section under a scanning electron microscope (Fig. 3c). The thickness of the composite is 175.5 ± 10.4 μm, and the fabric is mostly embedded in the matrix. Similarly, we prepare a composite of woven nylon fabric and PCU matrix.

We cut a sample in a rectangular shape, clamp the two long edges of the sample, and monotonically stretch the sample until rupture. We repeat the experiment with three materials: the neat PCU, the knit-PCU composite, and the weave-PCU composite (Fig. 4a). The modulus of the knit-PCU composite (∼10 MPa) is similar to that of the neat PCU matrix (∼7 MPa) and is much lower than that of the weave-PCU composite (∼100 MPa) (Fig. 4b). In this study, the ultimate stretch is defined as the stretch at maximum stress, reflecting the failure of the composite (Fig. S2, ESI†). The maximum stress for both the polycarbonate urethane (PCU) matrix and the knit composite is close to each other. This can be attributed to the strength of the knit fabric, which does not enhance the overall strength of the composite. The ultimate stretch of knit-PCU composite is smaller than that of the neat PCU but is much larger than that of the weave-PCU composite (Fig. 4c). Because the yarn in a knit structure is crimped, the knit-PCU composite has a low modulus and a large ultimate stretch. By contrast, because the yarns in a weave are nearly straight, the weave-PCU composite has a high modulus and a small ultimate stretch.

We stretch the knit-PCU composite under an optical microscope (Fig. 5). Define the stretch λ by the length of the deformed sample divided by the length of the undeformed sample. When $\lambda < 1.2$, the knit and the matrix are stretched concurrently. Neither the interface debonds, nor the yarn and matrix damage. In this stage, the stress–stretch curve of the composite is almost the same as that of PCU. The yarn curls and does not hinder the composite from deforming. When $1.2 < \lambda < 2$, the yarn debonds from the matrix and cuts the matrix, but the yarn itself does not break (Fig. S3, ESI†).

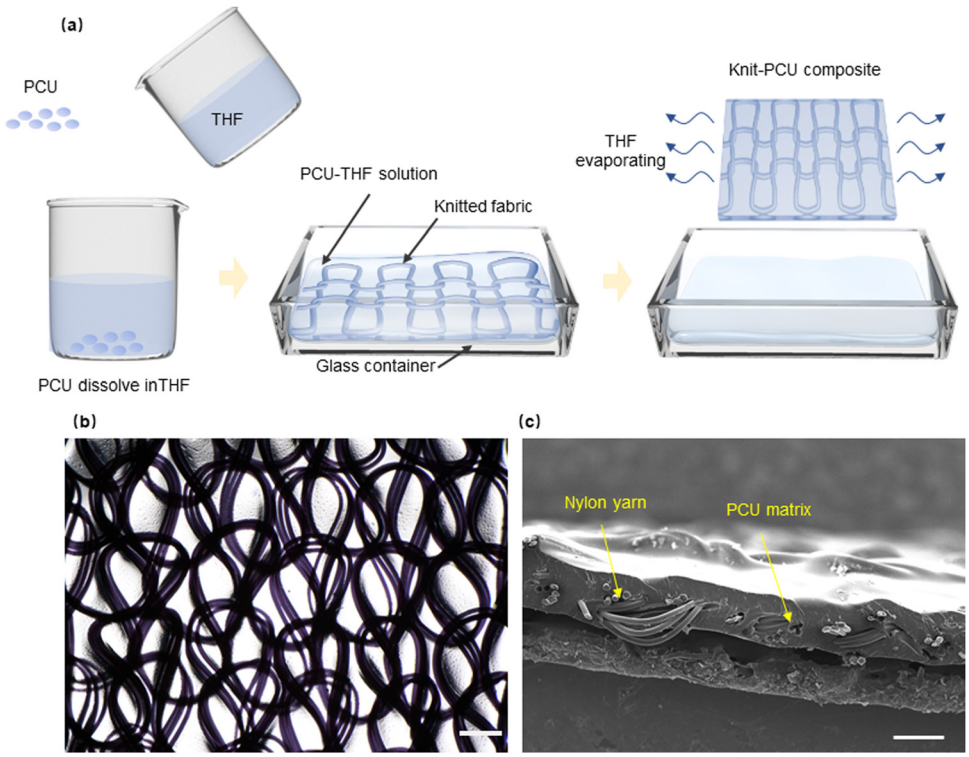

Fig. 3 (a) Fabrication of a knit-PCU composite. (b) Image of the composite in an optical microscope. Scale bar is 200 μm. (c) Image of the composite in a scanning electron microscope. Scale bar is 200 μm.

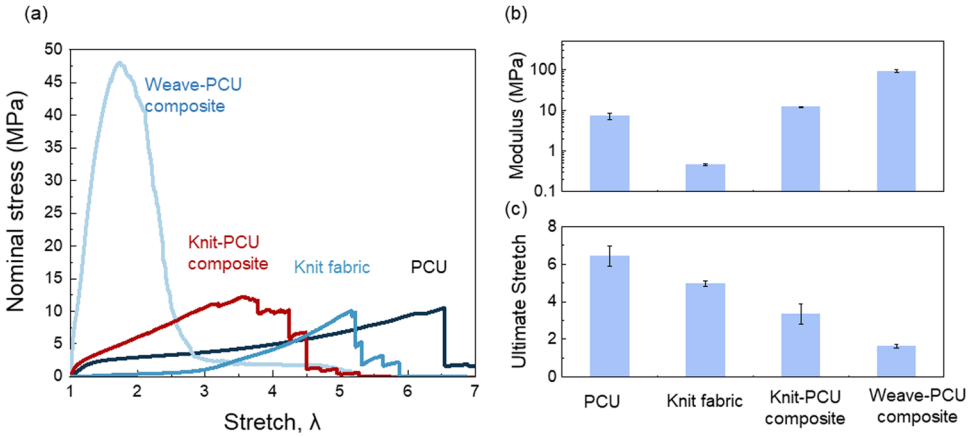

Fig. 4 (a) Stress–stretch curves of four materials: PCU, knit fabric, knit-PCU composite, and weave-PCU composite. (b) Moduli and (c) ultimate stretches of the three materials.

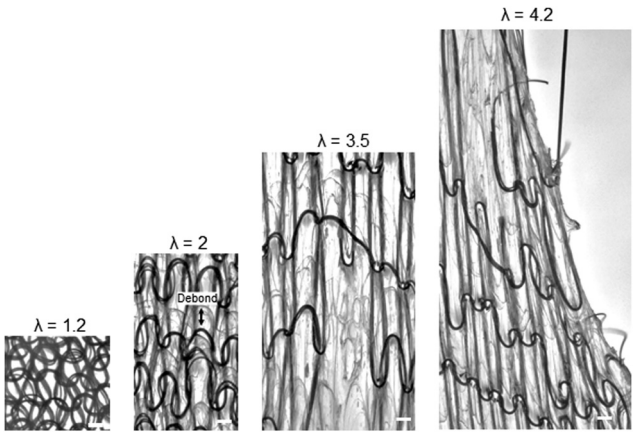

Fig. 5 Snapshots of a knit-PCU composite stretched under an optical microscope. Scale bars are 200 μm.

The yarn straightens to bear the load, so that the stress–stretch curve of the composite is above that of the neat PCU (Fig. 4a). The debond results in a channel in the matrix along the yarn (Movie S1, ESI†). When $\lambda > 3.5$, the yarn breaks, and large holes grow in the matrix till the sample separates into two parts.

4. Crack growth under monotonic stretch

We then stretch the knit-PCU composite with a precut crack (Fig. 6a and Movie S2, ESI†). When the sample is not stretched, $\lambda = 1$, the precut crack cuts the yarn, so that the crack edges roll. When $\lambda = 3$, the yarn slips, and the crack grows in the matrix. The yarn does not break, and the friction between the yarn and the matrix resists the crack growth. When $\lambda = 3.7$, the yarn breaks at a location ahead of the precut crack tip, and the crack grows substantially in the matrix. When $\lambda = 3.9$, the broken segment of the yarn still bridges the crack but bears little force. Meanwhile, the yarn ahead of the crack tip slips, and the crack grows further in the matrix. When $\lambda = 4.2$, the yarn breaks again at a location ahead of the crack tip, and the crack grows further in the matrix.

The stress–stretch curve is recorded during the test (Fig. 6b). The curve gradually rises to a peak. At the peak stress, the yarn breaks. The curve then descends in steps. Each step represents an additional yarn break. We convert the stretch to the energy release rate G by $G = HW(\lambda)$, where $W(\lambda)$ is the area under the stress–stretch curve of the intact sample, and H is the height of the sample.[16] The crack growth Δc is recorded using a microscope and is plotted as a function of the energy release rate (Fig. 6c). We identify two critical energy release rates G_A and G_B. The energy release rate at $\Delta c = 0$ is taken as G_A, which is 50 kJ m^{-2}. We take G_B as the peak energy release rate of the G–Δc curve, which is 170 kJ m^{-2}. When $G < G_A$, the yarn does not slip, and the crack does not grow in the matrix. When $G = G_B$, the yarn slips and breaks, and the crack grows in the matrix.

The processes of yarn slip and yarn break are illustrated schematically (Fig. 6d–f). The yarn slips against friction between the yarn and the matrix. As the yarn slips, the matrix also damages. The friction and the strength of the matrix together resist the yarn slip. The end of the yarn bears no force. Tension in the yarn builds up along the length of the yarn. If the friction is low and the matrix is weak, a long length of the yarn carries a low tension, and the yarn breaks at a location many loops ahead of the crack tip. If the friction is high and the matrix is strong, a short length of the yarn carries a high tension, and the yarn breaks at a location a few loops ahead of the crack tip. In our experiment, the yarn breaks at a location about 3–8 loops ahead of the crack tip.

5. Cyclic stretch

We subject samples without precut to cyclic stretch. Long rectangular shaped samples are stretched cyclically with a prescribed amplitude of stretch (Fig. 7a). The stress–stretch curve shows a large hysteresis loop in the first cycle (Fig. 7b).

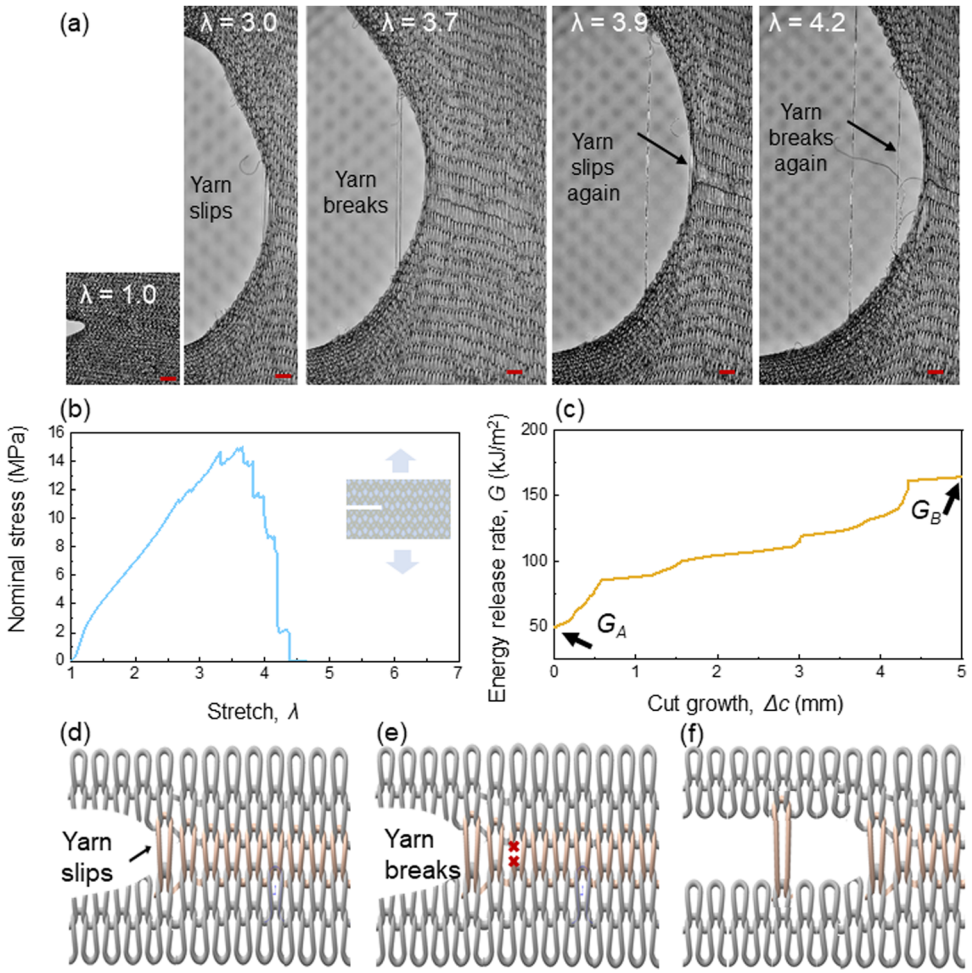

Fig. 6 (a) Snapshots at several stretches. Scale bar is 1 mm. (b) Stress–stretch curve of the knit-PCU composite with a precut crack. (c) The crack resistance curve. Schematic of (d) yarn slip, and (e) yarn break. (f) The processes repeat as the crack grows in the matrix.

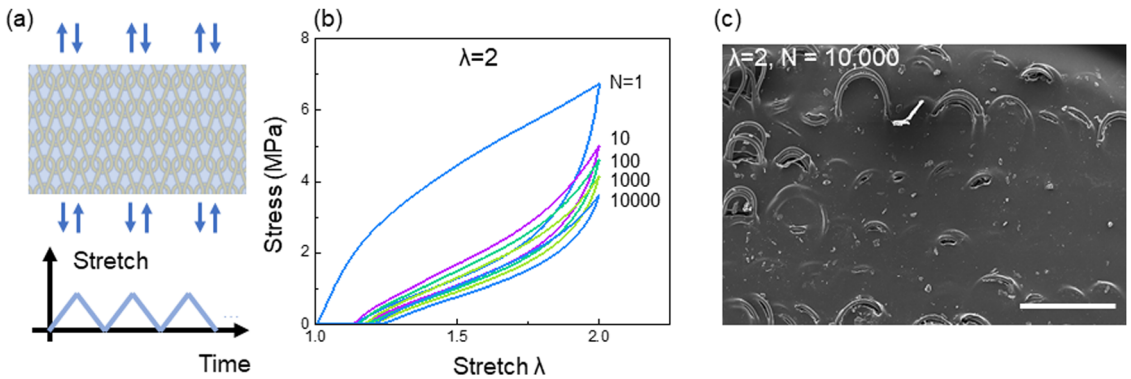

Fig. 7 A knit-PCU composite without precut crack under cyclic stretch. (a) Schematic of the cyclic test of the sample without precut. (b) Cyclic stress–stretch curve. (c) Scanning electron microscope image of the composite after 10 000 cycles. The scale bar is 500 μm.

After the first cycle, hysteresis becomes much smaller. The maximum stress drops from 6.74 MPa to 3.62 MPa after 10 000 cycles. In subsequent cycles, the stress–stretch curve changes negligibly. Before the test, the sample has a smooth surface and embeds the yarn inside. After the test, there are many cracks on the surface of the matrix, and the yarn is exposed (Fig. 7c). Cyclic stretch causes the yarn to cut the matrix repeatedly, and the interface debonds. The yarn/matrix debonding contributes to the observed hysteresis. In addition, we test the hysteresis of PCU matrix (Fig. S5, ESI†) and find

inherent viscoelasticity of the matrix also plays a significant role in the hysteresis.

We then subject a sample with a precut crack to cyclic stretch. The sample is of a long rectangular shape and is gripped along the long edges. For each cycle, the sample is loaded to a prescribed amplitude of stretch and is then unloaded until the crosshead returns to the initial position of the unstretched sample (Fig. 8a). The crack growth is plotted as a function of the number of cycles (Fig. 8b). Several samples are tested at various amplitudes of stretch. Depending on the amplitude of stretch, three types of behavior are identified. For a low amplitude of stretch, $\lambda = 1.3$, the crack does not grow in the matrix after 30 000 cycles. The tip of the precut crack shows negligible damage (Fig. 8c). For an intermediate amplitude of stretch, $\lambda = 2.0$, the crack grows in the matrix in the initial hundreds of cycles, and then arrests. Near the crack tip, the yarn slips out of the matrix cycle by cycle but does not break (Fig. 8d). The yarn slips against friction and bridges the crack. When the friction stops the yarn from slipping, the crack arrests. For a high amplitude of stretch, $\lambda = 3.0$, the crack grows unstopped as the yarn slips and breaks (Fig. 8e). When the yarn breaks in the bridging zone, the crack suddenly grows forward, a new bridging zone forms gradually under cyclic loading, and the yarn breaks again.

Recall that, after an intact sample is loaded for ~10 000 cycles, the stress–stretch curve changes negligibly and reaches a steady curve (Fig. 9b). Let $W_s(\lambda)$ be the area under the stress–stretch curve of the 10 000th cycle. We convert the amplitude of stretch to the amplitude of the energy release rate by $G(\lambda) = HW_s(\lambda)$.[17,18] We identify two thresholds of the amplitude of energy release rate, G_a and G_b. $G_a = 1.71$ kJ m^{-2} and $G_b = 12.13$ kJ m^{-2}. Here G_a is approximately the fatigue threshold of the neat PCU. When $G < G_a$, the crack cannot initiate even in the matrix. When $G_a < G < G_b$, the crack will grow and then arrest. When $G > G_b$, the crack will grow unstopped.

The slope of the c–N curve changes concurrently with the cyclic crack growth. We linearly fit the part of the c–N curve corresponding to the steady crack growth or arrest and record the slope as the crack growth rate dc/dN. The crack growth rate dc/dN increases with the energy release rate G (Fig. 9a). When the crack growth rate is less than 10^{-5} mm per cycle, we take the corresponding energy release rate as the threshold, that is $G_b = 12.13$ kJ m^{-2}. We take the length of crack growth before arrest as the arrest crack growth. When the arrest crack growth is less than 0.1 mm, we take the corresponding energy release rate as the threshold $G_a = 1.71$ kJ m^{-2}. The arrest crack growth increases with the energy release rate (Fig. 9b). It is noticed that the arrest crack growth (~10 mm) in the knit-PCU composite is very large compared to other materials, such as ceramics or a composite with epoxy matrix, where the crack arrests after propagating for <1 mm.[19–21]

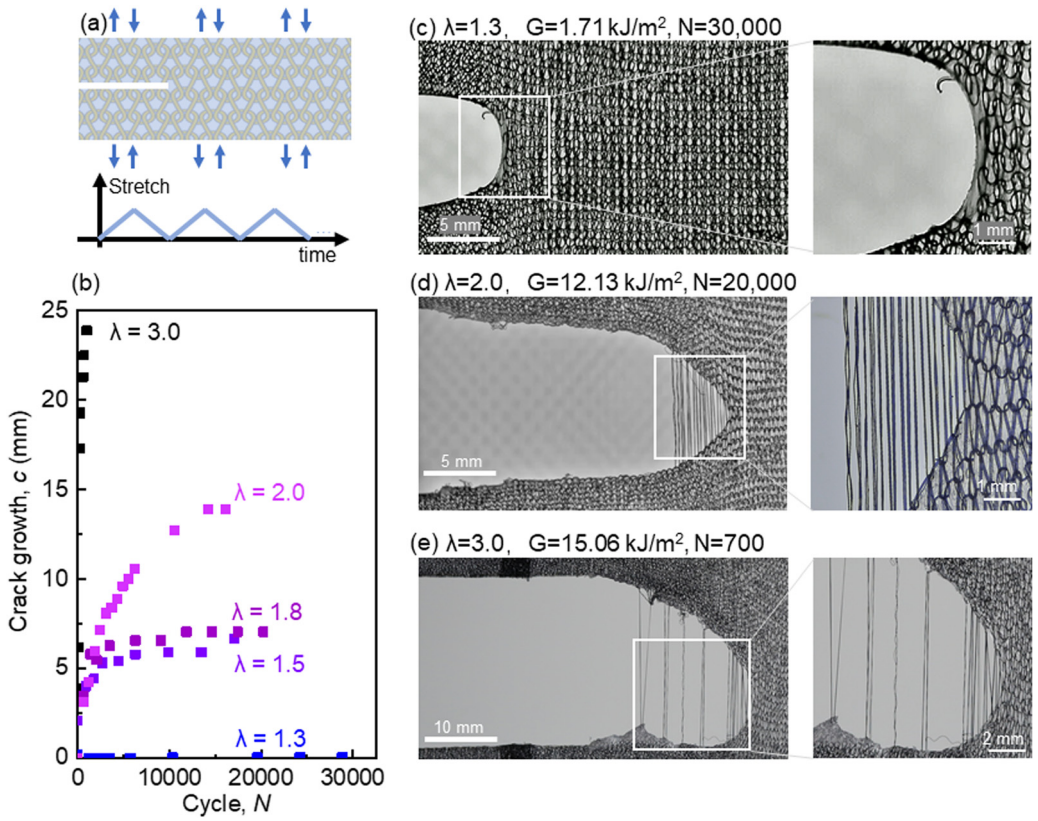

Fig. 8 Crack growth in the knit-PCU composite under cyclic stretch. (a) Schematic of the cyclic test of the sample with precut. (b) Crack growth as a function of the cycle number N. (c) Under a low amplitude of stretch, $\lambda = 1.3$, the crack does not grow. (d) Under an intermediate amplitude of stretch, $\lambda = 2.0$, the crack grows and arrests. (e) Under a high amplitude of stretch, $\lambda = 3.0$, the crack propagates continuously.

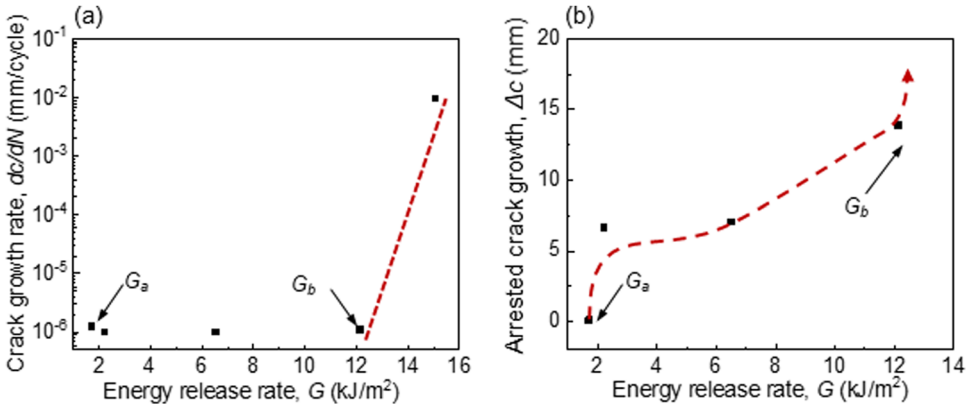

Fig. 9 Crack growth in a knit-PCU composite. (a) The crack growth rate dc/dN as a function of the energy release rate G. (b) The arrested crack growth after 20 000 cycles as a function of the energy release rate G.

6. Conclusions and discussion

We have studied the crack growth in the knit-PCU composite under both monotonic stretch and cyclic stretch. The crack grows in the matrix as the yarn slips and breaks. Under monotonic loading, we identify two critical energy release rates, G_A and G_B. When $G < G_A$, the yarn does not slip, and the crack does not grow in the matrix. When $G_A < G < G_B$, the yarn slips but does not break, and the crack grows in the matrix. The growth is stable in that the crack arrests when the load stops increasing. When $G = G_B$, the yarn slips and breaks, while the crack grows unstably. When the sample is subject to cyclic stretch, we observe analogous behavior of crack growth and arrest, as well as yarn slip and break. However, the two critical values, G_a and G_b, are much smaller than the corresponding values under monotonic load.

G_A and G_a represent the critical values for crack initiation. Under monotonic stretch, an energy release rate $G = G_A$ will cause cracks to initiate growth within the matrix, where the yarns start to slip. G_A is related to the toughness of the matrix and the yarn-matrix interface strength. Similarly, G_a under cyclic stretch relates to the fatigue threshold of the matrix and the interface endurance strength. Thus, the fact that G_a is much smaller than G_A is due to two factors: the fatigue threshold of the PCU being much lower than the toughness, and the interface endurance strength is much lower than the interface strength.[22,23]

G_B and G_b represent the critical values for yarn break. Under monotonic stretch, the yarn breaks when the tension in the yarn reaches the strength. G_B is related to the strength of the yarn and the strength of the interface.[24] Similarly, G_b is related to the yarn endurance strength and interface endurance strength (Fig. S4, ESI†). Both the yarn endurance strength and interface endurance strength are much lower than the yarn strength[25] and interface strength.[26] Thus, G_b is much lower than G_B.

In this study, we have examined crack growth in the course direction of a knitted fabric-reinforced composite. Future work will extend this investigation to the fracture behavior in the wale direction, where yarn laddering and breakage may play distinct roles in the crack propagation. Investigating the crack growth in this perpendicular direction will provide a more comprehensive view for the fracture of this composite. Polymer matrix exhibits temperature and rate-dependent properties that may affect the crack initiation and propagation behavior. Furthermore, four critical energy release rates are identified, with each corresponding to different failure modes. These energy release rates are influenced by factors such as yarn strength, interface strength, and matrix toughness. Understanding how these parameters affect the crack growth behavior enables more informed and targeted material design.

Author contributions

F. L. and X. C. designed the research. F. L. and X. C. carried out the experiments. J. T. and Z. S. supervised the work. All authors contributed to the writing of the paper.

Data availability

Data for this article, including curves and bar charts are available at Science Data Bank at **https://doi.org/10.57760/sciencedb.13605**.

Conflicts of interest

There are no conflicts to declare.

Acknowledgements

This research was supported by the National Natural Science Foundation of China (Grant no. 12422204). J. T. acknowledges the support of K. C. Wong Education Foundation.

Notes and references

1 P. Fratzl, *Collagen: structure and mechanics*, Springer, 2008, pp. 1–13.
2 I. Vesely, *J. Biomech.*, 1997, **31**, 115–123.
3 V. Ottani, M. Raspanti and A. Ruggeri, *Micron*, 2001, **32**, 251–260.
4 Y. J. No, M. Castilho, Y. Ramaswamy and H. Zreiqat, *Adv. Mater.*, 2019, **32**, e1904511.
5 L. Zeng, F. Liu, Q. Yu, C. Jin, J. Yang, Z. Suo and J. Tang, *Sci. Adv.*, 2023, **9**, eade7375.
6 W. Cui, Y. Huang, L. Chen, Y. Zheng, Y. Saruwatari, C.-Y. Hui, T. Kurokawa, D. R. King and J. P. Gong, *Matter*, 2021, **4**, 3646–3661.
7 W. Cui, D. R. King, Y. Huang, L. Chen, T. L. Sun, Y. Guo, Y. Saruwatari, C. Y. Hui, T. Kurokawa and J. P. Gong, *Adv. Mater.*, 2020, **32**, e1907180.
8 D. R. King, T. L. Sun, Y. Huang, T. Kurokawa, T. Nonoyama, A. J. Crosby and J. P. Gong, *Mater. Horiz.*, 2015, **2**, 584–591.
9 G. Zhang, T. Yin, G. Nian and Z. Suo, *Extreme Mech. Lett.*, 2021, **48**, 101434.
10 H. Fan and J. P. Gong, *Macromolecules*, 2020, **53**, 2769–2782.
11 X. P. Ruan and T. W. Chou, *Compos. Sci. Technol.*, 1996, **56**, 1391–1403.
12 S. Poincloux, M. Adda-Bedia and F. Lechenault, *Phys. Rev. X*, 2018, **8**, 021075.
13 R. Chang, Z. Chen, C. Yu and J. Song, *J. Appl. Mech.*, 2019, **86**, 011012.
14 T. J. Dann, D. J. Carr, R. M. Laing, B. E. Niven and J. Kieser, *Forensic Sci. Int.*, 2012, **217**, 93–100.
15 W. P. Moestopo, S. Shaker, W. Deng and J. R. Greer, *Sci. Adv.*, 2023, **9**, eade6725.
16 R. S. Rivlin and A. G. Thomas, *J. Polym. Sci.*, 2003, **10**, 291–318.
17 R. Bai, Q. Yang, J. Tang, X. P. Morelle, J. Vlassak and Z. Suo, *Extreme Mech. Lett.*, 2017, **15**, 91–96.
18 W. Zhang, J. Hu, J. Tang, Z. Wang, J. Wang, T. Lu and Z. Suo, *ACS Macro Lett.*, 2019, **8**, 17–23.
19 L. Ewart and S. Suresh, *J. Mater. Sci.*, 1987, **22**, 1173–1192.
20 T. T. Shih and J. Opoku, *Eng. Fract. Mech.*, 1979, **12**, 479–498.
21 Y. Charles and F. Hild, *Int. J. Fract.*, 2002, **115**, 251–272.
22 G. Scetta, E. Euchler, J. Ju, N. Selles, P. Heuillet, M. Ciccotti and C. Creton, *Macromolecules*, 2021, **54**, 8726–8737.
23 G. Scetta, N. Selles, P. Heuillet, M. Ciccotti and C. Creton, *Polym. Test.*, 2021, **97**, 107140.
24 M. D. Thouless and A. G. Evans, *Acta Metall.*, 1988, **36**, 517–522.
25 P. Alam, D. Mamalis, C. Robert, C. Floreani and C. M. Ó. Brádaigh, *Composites, Part B*, 2019, **166**, 555–579.
26 F. Liu, Z. Suo and J. Tang, *J. Mech. Phys. Solids*, 2022, **158**, 104659.